The chemistry of the NO/NO$_2$–NH$_3$ "fast" SCR reaction over Fe-ZSM5 investigated by transient reaction analysis

Antonio Grossale [a], Isabella Nova [a], Enrico Tronconi [a,*], Daniel Chatterjee [b], Michel Weibel [b]

[a] *Dipartimento di Energia, Laboratorio di Catalisi e Processi Catalitici, Politecnico di Milano, Piazza Leonardo da Vinci 32, I-20133 Milano, Italy*
[b] *Daimler AG, Abteilung GR/VPE, D-70546 Stuttgart, Germany*

ABSTRACT

We present a systematic study of the chemical steps in the NO/NO$_2$–NH$_3$ fast SCR reaction 2NH$_3$ + NO + NO$_2$ → 2N$_2$ + 3H$_2$O over a commercial Fe-ZSM5 catalyst. The study is based on transient reaction experiments at realistic conditions for removal of NO$_x$ from mobile diesel exhausts. Its goal is to assess and critically evaluate the current ideas on the SCR mechanism, and also to establish to what extent the mechanistic pathways demonstrated for V-based catalysts also apply to Fe-promoted zeolites. Results show that the fast SCR reaction proceeds at low temperature via a global sequence involving NH$_4$NO$_3$ or related surface species as intermediates,

$$2NO_2 + 2NH_3 \rightarrow N_2 + NH_4NO_3 + H_2O,$$

$$NO + NH_4NO_3 \rightarrow NO_2 + N_2 + 2H_2O.$$
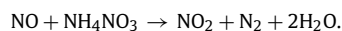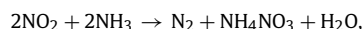
Such a sequential scheme is the same as that proposed previously for the fast SCR chemistry over V-based catalysts and other zeolite catalysts and thus is considered a general mechanism. It explains all of the available observations for stoichiometry (e.g., optimum NO/NO$_2$ unit molar ratio), selectivity (e.g., N$_2$O from NH$_4$NO$_3$ decomposition), and kinetics (e.g., rate of fast SCR = rate of nitrate reduction by NO). We further show that the redox reaction between NO and nitrates is the rate-controlling step and is inhibited by ammonia. Remarkably, the same strongly enhanced deNO$_x$ activity observed in the fast SCR reaction also was observed in the absence of gaseous NO$_2$ but in the presence of surface nitrates. We accordingly propose a general summary of the fast SCR chemistry over V-based and zeolite catalysts that emphasizes the key role of surface nitrates.
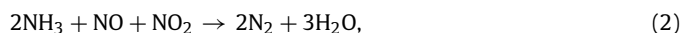
1. Introduction

In addition to the well-known "standard" SCR reaction,

$$2NH_3 + 2NO + \frac{1}{2}O_2 \rightarrow 2N_2 + 3H_2O, \tag{1}$$
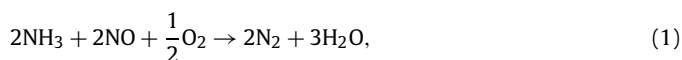
the so-called "fast" SCR reaction,

$$2NH_3 + NO + NO_2 \rightarrow 2N_2 + 3H_2O, \tag{2}$$

plays a critical role at 180–300 °C in boosting the denitrification (deNO$_x$) activity of new generation urea-SCR converters for diesel vehicles integrated with an upstream preoxidation catalyst that partially oxidizes NO to NO$_2$ [1].

Koebel and co-workers [1–4] first extensively investigated the fast SCR reaction over V$_2$O$_5$–WO$_3$/TiO$_2$ SCR catalysts. To explain the higher rate of the fast SCR reaction, they proposed a redox mechanism in close analogy with that of the standard SCR reaction, but with NO$_2$ serving as a more efficient oxidizing agent for the vanadium sites than oxygen [3]. Furthermore, for the NO–NO$_2$/NH$_3$ reacting system, they also reported the occurrence at low temperatures of two side reactions not observed in the presence of NO–NH$_3$ only—namely the formation of ammonium nitrate,

$$2NH_3 + 2NO_2 \rightarrow NH_4NO_3 + N_2 + H_2O, \tag{3}$$
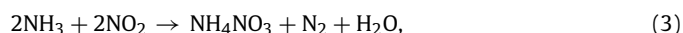
and the decomposition of ammonium nitrate by NO, described according to the following stoichiometry [4]:

$$NH_4NO_3 \leftrightarrow NH_3 + HNO_3, \tag{4}$$

$$2HNO_3 + NO \rightarrow 3NO_2 + H_2O. \tag{5}$$

However, reactions (3)–(5) were considered to be side reactions occurring in parallel to fast SCR (1), not participating in its mechanism [4].

In our work aimed at developing a chemically consistent simulation model of SCR converters for automotive applications [5], we have addressed mechanistic aspects of the fast SCR chemistry

over commercial vanadium-based catalysts by means of transient reaction analysis [6–10]. Our data have shown that the fast SCR chemistry proceeds over V_2O_5–WO_3/TiO_2 SCR catalysts at low temperature via a sequential scheme, which can be summarized as comprising two global reactions—ammonium nitrate formation [reaction (3)] and the following reaction between ammonium nitrate and NO—formally involving NH_4NO_3 as an intermediate:

$$NH_4NO_3 + NO \rightarrow NO_2 + N_2 + 2H_2O. \qquad (6)$$
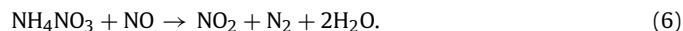
In fact, the sum of (3) and (6) yields the stoichiometry of the fast SCR reaction (2). Notably, reactions (3) and (6) are similar to those already reported by Koebel and co-workers, but here they are not just side reactions, but are intimately related to the fast SCR chemistry.

The mechanism of the first step in the fast SCR sequential scheme—ammonium nitrate formation [reaction (3)]—was clarified by Koebel's group [1–4] and implies NO_2 dimerization (7), disproportion (8), and successive reactions between nitrous and nitric acid and NH_3 (9), (10), with rapid decomposition of ammonium nitrite to nitrogen:

$$2NO_2 \leftrightarrow N_2O_4, \qquad (7)$$

$$N_2O_4 + H_2O \leftrightarrow HONO + HNO_3, \qquad (8)$$

$$NH_3 + HONO \leftrightarrow NH_4^+ + NO_2^- \leftrightarrow [NH_4NO_2] \rightarrow N_2 + 2H_2O, \qquad (9)$$

$$NH_3 + HNO_3 \leftrightarrow NH_4^+ + NO_3^- \leftrightarrow NH_4NO_3. \qquad (10)$$
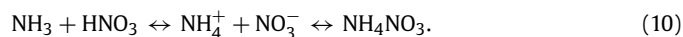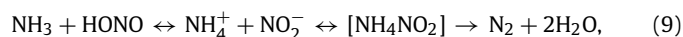
Concerning the second step in the fast SCR sequential scheme—reaction (6) between NO and ammonium nitrate—we have demonstrated by dedicated transient experiments a mechanism based on: ammonium nitrate decomposition (10 reverse), successive oxidation of NO to NO_2 by nitric acid, which is thus reduced to nitrous acid (11), and reaction of the latter with NH_3 to form N_2 via ammonium nitrite decomposition (9) [6–10]:

$$NH_4NO_3 \leftrightarrow NH_3 + HNO_3, \qquad (4) = (10\text{ reverse})$$

$$HNO_3 + NO \leftrightarrow NO_2 + HONO, \qquad (11)$$

$$NH_3 + HONO \rightarrow N_2 + 2H_2O. \qquad (9)$$

We further observed that the rate-limiting step (6) does not proceed over V-free WO_3/TiO_2 and thus is catalyzed by V_2O_5. The same results had been previously reported for reaction (5) [4]. According to a redox interpretation of the fast SCR chemistry over V-based catalysts, the key global reaction (6) actually is associated with a redox cycle involving the more effective reoxidation of reduced V-sites by surface nitrates [8,9]; the fast SCR activity of NO/NO_2–NH_3 is similar to the activity of NH_3 + NO in the absence of gaseous NO_2 but in the presence of either NH_4NO_3 [6,7,10] or nitrates prestored onto the vanadium catalyst surface [8,9]. This rules out the possibility that the fast SCR reaction (2) can proceed in parallel or consecutively to the nitrate decomposition by NO [reaction (6)].

There is now a trend in the automobile industry to replace vanadium-based SCR catalysts with zeolite-based systems to expand the operating temperature window and address the problems associated with high-temperature deactivation of the anatase–rutile TiO_2 transition. Zeolites are the new class of automotive SCR catalysts. Various zeolites have been proposed for this purpose, including ZSM-5, mordenite, beta, ferrierite, and Y-zeolite [11]. In the most active systems, zeolites generally are promoted by transition metals, such as iron, copper, and silver. These catalysts reportedly are associated with good deNO$_x$ activity in the standard and especially the fast SCR reactions [11–17].

Concerning the mechanistic features of fast SCR over zeolites, Weitz et al. [18] proposed a fast SCR pathway over a BaNa–Y zeolite similar to that discussed above for V_2O_5–WO_3/TiO_2 catalysts,

based on spectroscopic evidence and on steady-state reaction data. In addition, other authors have reported NO_2 disproportion [19–21] and ammonium nitrate formation [16,22] over promoted and unpromoted zeolites. Based on the analysis of their own data and of literature data, Kröcher et al. [23] recently proposed a common SCR reaction scheme for transition–metal zeolites and for vanadium-based catalysts that is in close agreement both with the chemistry over a V_2O_5–WO_3/TiO_2 catalyst reported in our previous work [6,7] and with the scheme proposed for the BaNa–Y zeolite [18].

Herein we present a dedicated investigation of the elementary steps of the fast SCR reaction at low temperature over the same commercial Fe-ZSM5 catalyst used in a previous SCR reactivity study [26]. Our goal is to assess and critically evaluate the current ideas on the SCR mechanism, and specifically to establish in a conclusive manner to what extent the same mechanistic pathways demonstrated for V-based catalysts also apply to Fe-promoted zeolite catalysts under fully representative conditions for automotive applications. For this purpose, we take the same experimental approach (transient reaction experiments) used in our previous mechanistic investigation over V_2O_5–WO_3/TiO_2, in order to establish a direct link to the results for V-based catalysts.

2. Experimental

The commercial catalyst used in this work was originally supplied by Daimler in the form of a cordierite honeycomb monolith (400 cpsi—6.5 mils) washcoated with Fe-ZSM5. For testing, the catalyst was crushed and sieved to 140–200 mesh, to avoid mass transfer limitations. Samples (160 mg of catalyst powder or 80 mg of catalyst powder diluted with 80 mg of quartz powder) were loaded into a flow-microreactor consisting of a quartz tube (6 mm i.d.) placed in an electric furnace. The reaction temperature was monitored and controlled by a K-type thermocouple immersed in the catalyst bed. Mass-flow controllers (Brooks Instruments) were used to dose He, Ar, NH_3, NO, NO_2, and O_2 in the gaseous feed stream, while water vapor was added via a saturator operated at controlled temperature. All of the lines before and after the reactor were heated to 200 °C to prevent H_2O condensation and NH_4NO_3 deposition. The species concentrations in the outlet stream were continuously monitored by a quadrupole mass spectrometer (Balzer QMS 200) and a UV analyzer (ABB-LIMAS 11 HV) in parallel. He was used as carrier gas to enable evaluation of N balances at steady state. More experimental details are available elsewhere [5,7,8,26].

Before the experiments, the catalyst was conditioned with a temperature ramp of 10 °C/min up to 600 °C in 2% O_2 v/v, then held at 600 °C for 1 h. Transient runs consisted of step-response experiments at 150–170–190 °C (transient response method [TRM]) and in temperature-programmed reaction (TPR) runs. In a typical TRM run, the reactor was kept at constant temperature under a flow of He + 1% H_2O, and step changes (e.g., $0 \rightarrow 1000 \rightarrow 0$ ppm or $0 \rightarrow 500 \rightarrow 0$ ppm) of feed NH_3 or NO or NO_2 concentrations were imposed. TRM tests were carried out over diluted catalyst beds at 72 or 140 cm³/min (STP), corresponding to GHSV = 8600–23,000 h^{-1} if referred to a monolith catalyst. At the end, a temperature ramp (10 °C/min, $T_{end} = 550$ °C) was run to clean up the catalyst surface. In the TPR runs, a stream containing NH_3 (1000 ppm) and NO_x (1000 ppm, with NO/NO_x = 1 or 0.5) with O_2 (0 or 2% v/v) and H_2O (1% v/v) in He was fed to the reactor initially at 150 °C, and then the reactor temperature was linearly increased up to 550 °C at a heating rate of 20 °C/min. Because the purpose of this work was to address the chemistry of the fast SCR reaction (2), many runs were performed in the absence of O_2 so as to eliminate contributions of the standard SCR reaction (1).
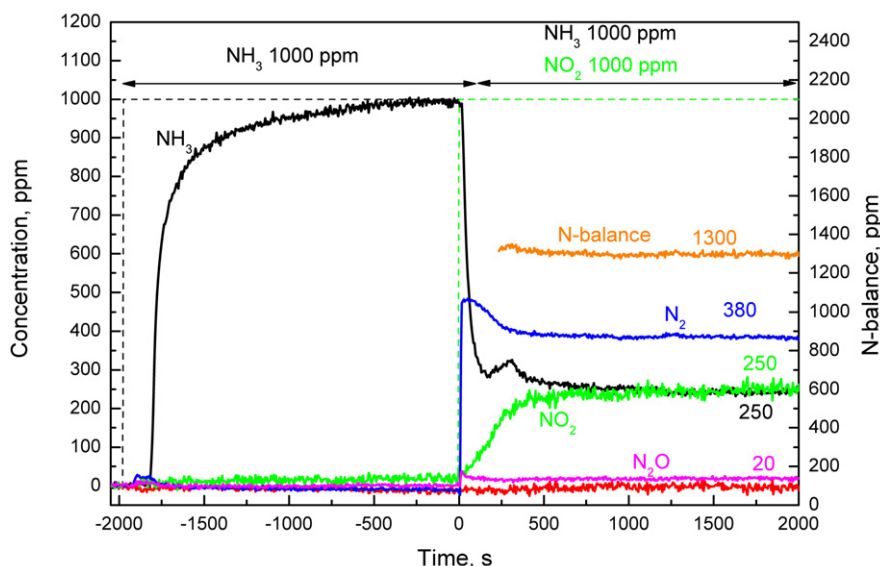
Fig. 1. Formation of ammonium nitrate over the Fe-ZSM5 catalyst. $W_{cat} = 0.080$ g, flow rate = 140 cm^3/min (STP). Feed = 1% H_2O, 2% O_2, 1000 ppm NH_3 and 1000 ppm NO_2 + He. $T = 180\,^{\circ}$C.

Additional NO_2 adsorption runs were performed to study the formation of surface nitrates and NH_4NO_3 over undiluted crushed monolith samples at 120 cm^3/min (STP). A few final runs with step changes in the NH_3 feed were devoted to study the fast SCR dynamics over Fe-ZSM5 at 200 °C using a higher feed flow rate (240 cm^3/min STP) in the presence of O_2 (2%), to extend the study to conditions closer to automotive applications.

3. Results and discussion

3.1. NH_4NO_3 formation

Fig. 1 shows a transient run at 180 °C addressing the formation of ammonium nitrate over Fe-ZSM5. After the catalyst was saturated with NH_3 (1000 ppm), at time $t = 0$ s NO_2 (1000 ppm) was added stepwise to the feed stream. At steady state, the data indicate equal conversions of NO_2 and NH_3 ($\Delta NO_2 = \Delta NH_3 = 750$ ppm), the formation of N_2 (380 ppm), of N_2O (20 ppm), and a lack of about 700 ppm in the overall N balance (total atomic $N = 1300$ ppm). These results agree with the stoichiometry of reaction (3) and correspond to the formation of about 350 ppm of NH_4NO_3, which, of course, cannot be detected by our analyzers. In previous work [6,7,10], we found similar behavior (except for N_2O formation) over a V_2O_5–WO_3/TiO_2 catalyst and also documented that part of the NH_4NO_3 was decomposed to HNO_3 + NH_3 and escaped undetected from the reactor, later condensing in cold spots along the downstream lines.

As discussed above, in the case of V-based catalysts and BaNa–Y zeolites, the formation of ammonium nitrate has been attributed in the past to NO_2 dimerization and disproportion [reactions (7) and (8)], coupled with the formation and decomposition of ammonium nitrite [reaction (9)] and the reaction between nitric acid and ammonia [reaction (10)]. We addressed the question as to whether the same mechanism also applies to Fe-ZSM5 by means of two NO_2 adsorption experiments conducted at 150 °C in the absence and presence of preadsorbed NH_3 (Figs. 2A and 2B). Both runs consist of a step addition of NO_2 only (1000 ppm at $t = 0$ s) to a feed stream containing 1% H_2O, 2% O_2, and He flowing over either a clean Fe-ZSM5 catalyst or a catalyst sample previously exposed to NH_3 at 150 °C.

Fig. 2A shows storage of NO_2 onto the catalyst up to saturation in the absence of preadsorbed ammonia, accompanied by evolution of NO. The data, reported previously [26], are consistent with

$$3NO_2 + H_2O \leftrightarrow NO + 2HNO_3. \qquad (12)$$
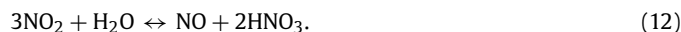
Note that the molar ratio $NO/\Delta NO_2$ is approximately equal to 1/3 during the entire adsorption transient. The overall reaction (12) actually describes the chemisorption of NO_2 in the form of nitrates and results from the combination of the NO_2 dimerization and disproportion reactions [reactions (7) and (8)] and the oxidation of nitrite species by NO_2 [reaction (11 reverse)]. Accordingly, the results of Fig. 2A agree with the proposed chemistry and with IR studies documenting the formation of nitrates on zeolite catalysts on exposure to NO_2 [18,24,25]. Kröcher and co-workers also demonstrated reaction (12) in relation to NO_2 adsorption onto Fe-ZSM5 [22] and Cu-ZSM5 [21].

When the same NO_2 storage experiment was run in the presence of ammonia preadsorbed on the catalyst, however, evolution of N_2 instead of NO was observed, as shown in Fig. 2B. Remarkably, the N_2 concentration detected during the initial stage of the reaction amounted to about 500 ppm versus a total conversion of the 1000 ppm of NO_2 in the feed. This corresponds to the overall stoichiometry of ammonium nitrate formation from NO_2 and adsorbed ammonia [reaction (3)], according to steps (7)–(10), which involve disproportion of NO_2 [reactions (7) and (8)], as shown in Fig. 2A, but in this case followed by reaction of nitrites with NH_3 rather than with NO_2 and leading to N_2 via ammonium nitrite decomposition [reaction (9)]. As a further confirmation, we note that the total amount of N_2 evolved during the experiment in Fig. 2B ($\approx$0.2 mmol/g) was close to the amount of preadsorbed ammonia ($\approx$0.18 mmol/g), as would be expected from (9). A TPD run at the end of the NO_2 storage phase demonstrated no N_2O evolution, thus confirming that no NH_4NO_3 was left on the catalyst. On the other hand, the NO_2 evolution from nitrate decomposition was similar to that observed during the corresponding final TPD part of the run shown in Fig. 2A.

Comparing the chemistry involved in NO_2 adsorption onto Fe-ZSM5 in the absence and in the presence of adsorbed ammonia reveals that at 150 °C surface nitrites (or nitrous acid) react more readily with NH_3 according to the ammonium nitrite formation/decomposition reaction (9) rather than with NO_2 according to the reverse of (11), the reaction observed in the absence of am-
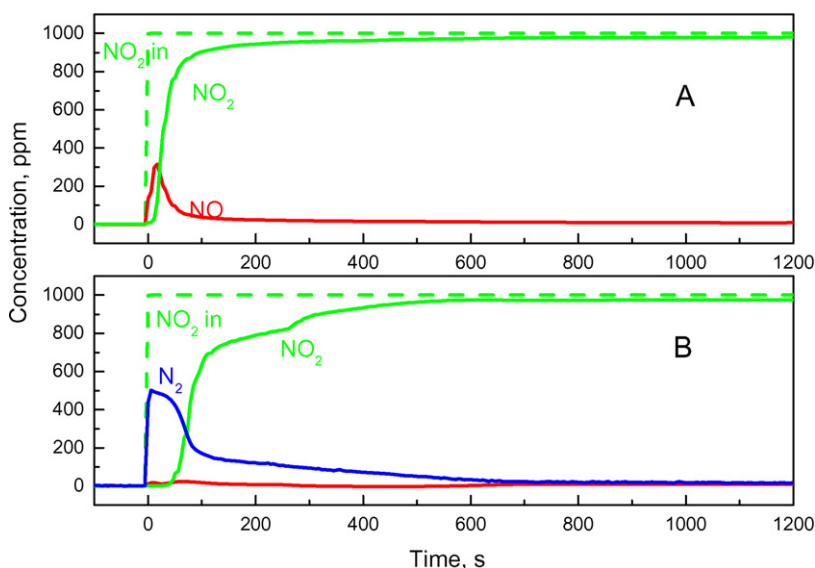
Fig. 2. Effect of preadsorbed NH_3 on NO_2 storage on Fe-ZSM5. $W_{cat} = 0.160$ g, flow rate $= 120$ cm^3/min (STP). Feed $= 1\%$ H_2O, 2% O_2, $NO_2 = 1000$ ppm $+$ He. $T = 150\,^\circ$C. A $=$ clean catalyst. B $=$ catalyst with preadsorbed NH_3.

monia. This reaction is indeed very fast; complete oxidation of nitrous acid by NO_2 occurs already at $150\,^\circ$C, as indicated by the stoichiometry observed during NO_2 adsorption on the clean catalyst (see Fig. 2A and related discussion). Other data (not reported) show the same behavior already at $50\,^\circ$C. Thus, the preferential reaction of nitrites with ammonia, even if their oxidation by NO_2 is so facile, merits some consideration. Our data also indicate that ammonia reacts preferentially with surface nitrites, thus forming N_2, rather than with nitrates to form NH_4NO_3.

3.2. Reactivity of NH_4NO_3 with NO

To investigate the reactivity of NH_4NO_3 with nitric oxide over Fe-ZSM5, ammonium nitrate was generated in situ (i.e., on the catalyst itself). As shown in Fig. 3, 1000 ppm of NO_2 along with H_2O (1% v/v) and O_2 (0% v/v) were initially fed to the microreactor at $170\,^\circ$C; subsequently, 1000 ppm of NH_3 was added to the feed to form and build up ammonium nitrate on the catalyst surface according to reaction (3). At the end of the first build-up stage, only NO_2 was removed from the feed stream while NH_3 was retained, to limit decomposition of ammonium nitrate to $NH_3 + HNO_3$, thus preserving a significant fraction of the ammonium nitrate formed on the catalyst. In the final stage of the run, 1000 ppm of NO was added to the NH_3-containing feed stream, still without oxygen. The same experimental procedure has been used previously to study the reactivity of NH_4NO_3 with nitric oxide over V_2O_5–WO_3/TiO_2 [6,7].

Fig. 3 shows the temporal evolutions of the outlet concentrations of NH_3, NO, NO_2, N_2, and N_2O during the NH_4NO_3 buildup and reactivity run over Fe-ZSM5. During the first stage ($t < 7600$ s), when NH_3 and NO_2 were co-fed to the reactor, a roughly equimolar consumption of both species was observed ($\Delta NO_2 = 830$ ppm; $\Delta NH_3 = 820$ ppm), along with formation of 430 ppm of N_2, 15 ppm of N_2O, and a lack of 760 ppm in the N balance (total atomic $N = 1240$ ppm). Such results are clearly in line with the formation of ammonium nitrate [reaction (1)], as discussed in the previous section, and point to the formation/deposition of NH_4NO_3 salt onto the catalyst surface. A small fraction of such ammonium nitrate was decomposed to N_2O. The formation of NH_4NO_3 salt on V_2O_5–WO_3/TiO_2 under similar conditions has been documented by IR analysis of a catalyst sample unloaded from the reactor [10].

After the NO_2 feed was shut off, the ammonia concentration level returned to its feed value, and the concentrations of all the other species dropped to zero. This indicates that no reaction occurred between ammonia and ammonium nitrate at this temperature [6,7,10]. At $t = 9600$ s, NO (1000 ppm) was added to NH_3 in the feed, which resulted in a long transient (prolonged until $t \approx 13{,}000$ s), associated with the conversion of NO and NH_3 and the formation of N_2 and NO_2. The conversion ratio of NO and NH_3 was 1:1 during the entire transient period except the initial 600 s, when a higher NO consumption along with formation of a few ppm of NO_2 were seen. The evolution of nitrogen mirrored the consumption of NO and NH_3 but exceeded it significantly (e.g., $\Delta NO = 90$ ppm, $\Delta NH_3 = 100$ ppm, $N_2 = 130$ ppm).

The reactivity observed when NH_3 and NO were co-fed to the Fe-ZSM-5 catalyst cannot be explained by the standard SCR reaction (1), which exhibits a different stoichiometry and requires the participation of O_2. Rather, it is attributed to the reaction (6) between NO and the ammonium nitrate deposited onto the catalyst during the previous stage of the experiment. Under similar operating conditions, we observed the same behavior over a V_2O_5–WO_3/TiO_2 catalyst; we explain this as due to the following reaction:

$$NH_3 + NO + \frac{1}{2}NH_4NO_3 \rightarrow \frac{3}{2}N_2 + \frac{5}{2}H_2O. \tag{13}$$
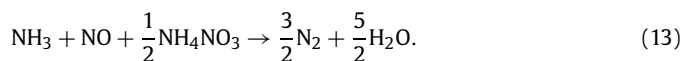
In view of the 1:1 consumption ratio between NO and NH_3, along with the formation of about 3/2 ppm of N_2 for each ppm of converted NO observed over Fe-ZSM5, reaction (13) also explains the results shown in Fig. 3. Notably, reaction (13) is simply the sum of reaction (6) between NO and ammonium nitrate, forming NO_2, and reaction (3) between such NO_2 and NH_3, which rapidly reforms part of the converted ammonium nitrate.

Additional runs to explore the temperature dependence of the reactivity of NH_4NO_3 with NO were performed at 150 and $190\,^\circ$C (Figs. 4A and 4B). At both temperatures, the Fe-ZSM5 catalyst was active in the formation of ammonium nitrate [reaction (3)], confirming the expected stoichiometry within experimental error. An increase in the associated NO_2 and NH_3 conversions was observed with decreasing temperature, indicating that NH_4NO_3 formation is favored by low temperatures, in agreement with the literature [1,18]. As for the reaction between ammonium nitrate and NO $+$ NH_3, no conversion was apparent at $150\,^\circ$C (Fig. 4A), whereas considerable reactivity was detected at $190\,^\circ$C (Fig. 4B). In fact, in

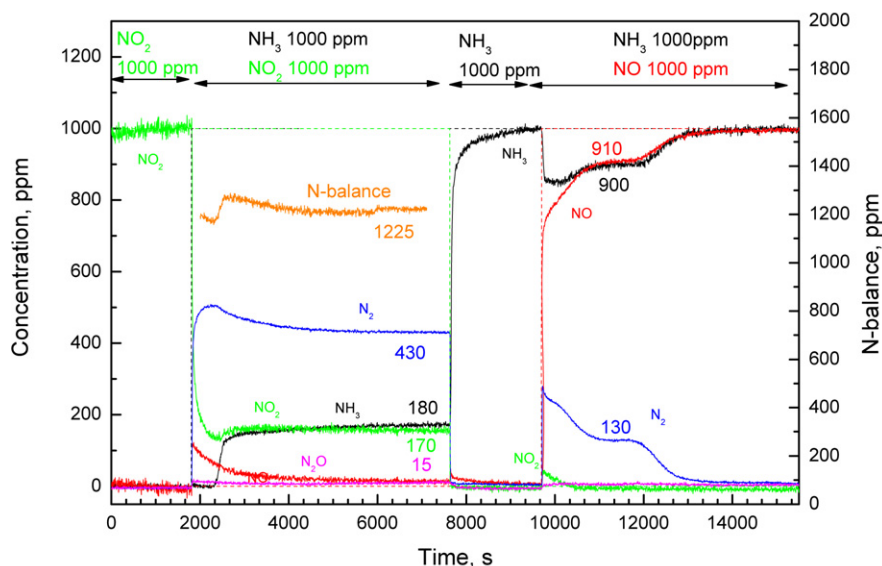**Fig. 3.** Buildup of ammonium nitrate and its reactivity with NO over Fe-ZSM5. $W_{cat} = 0.080$ g, flow rate = 72 cm^3/min (STP). Feed = 1% H$_2$O, 0% O$_2$, NH$_3$ = 0–1000 ppm, NO = 0–1000 ppm, NO$_2$ = 0–1000 ppm + He. $T = 170$ °C.

the latter case, an initial evolution of 450 ppm of N$_2$ was found, which is in fair agreement with reaction (13) (ΔNO = 320 ppm) but far greater than the 130 ppm of N$_2$ observed in the run at 170 °C (Fig. 3).

Based on the aforementioned findings, it seems legitimate to conclude that a similar reactivity between NO and ammonium nitrate applies over the present Fe-ZSM5 catalyst, as has been reported previously for V$_2$O$_5$–WO$_3$/TiO$_2$ catalysts and a BaNa–Y zeolite [6,7,18,23]. The results shown in Fig. 3 and the related interpretation also agree with the IR data of Busca et al. [25], who studied the interaction of NO and NO/NO$_2$ with NH$_3$ preadsorbed onto H-ZSM5 and found that NO$_2$ reacted readily at room temperature with adsorbed ammonium ions, forming nitrates and N$_2$, as expected from reaction (3), whereas in the presence of NO + NO$_2$, the catalyst was completely depleted of adsorbed ammonia and of nitrates at 373 K, consistent with the reduction of nitrates by NO [reaction (11)] and the resulting overall reaction (2). Furthermore, the present data demonstrate a strong temperature dependence of reaction (6) between NO and NH$_4$NO$_3$.

3.3. Role of NH$_4$NO$_3$ in the fast SCR reaction

After demonstrating the reactivity of NH$_4$NO$_3$ with NO over Fe-ZSM5, we proceeded to study the relationship of such a reaction with the NO/NO$_2$–NH$_3$ (fast SCR) reacting system. In analogy with our previous studies on a V-based catalyst [6,7], the study relied on TRM runs involving a first stage in which NH$_3$, NO, and NO$_2$ (1000:500:500 ppm) were co-fed to the Fe-ZSM5 catalyst along with H$_2$O (1% v/v) but with no O$_2$, followed by a second stage after stepwise removal of NO$_2$ from the feed stream.

Fig. 5 displays the dynamics of the NH$_3$, NO, NO$_2$, N$_2$, and N$_2$O outlet concentrations observed during one of such runs at 170 °C. At $t > 3000$ s, when NO and NO$_2$ were added to NH$_3$ in the feed, a reaction transient associated with conversion of both NH$_3$ and NO$_x$ and with the formation of N$_2$ and of a few ppm of N$_2$O became apparent. At steady state, the NH$_3$ consumption was around 440 ppm, close to the NO$_x$ conversion of 460 ppm. It should be noted, however, that the NO$_2$ conversion was much greater than the NO conversion (ΔNO = 40 ppm, ΔNO$_2$ = 420 ppm); therefore, the fast SCR reaction (2) by itself cannot explain the observed behavior, because it would result in equimolar conversions of NO and NO$_2$. In view of the low temperature (170 °C) and of the higher

NO$_2$ conversion, it is then reasonable to propose that also reaction (3) (i.e., formation of ammonium nitrate) also was proceeding along with the fast SCR reaction (2). The formation of NH$_4$NO$_3$ is in fact corroborated by a lack in the atomic nitrogen balance at steady state; furthermore, it is compatible with the observed N$_2$ concentrations, as we briefly discuss in what follows.

We consider the NO consumption (ΔNO = 40 ppm) to represent the extent of the fast SCR reaction (2), whereas the extent of reaction (3) is obtained by subtracting the amount of NO converted by the fast SCR reaction from the total NO$_2$ conversion: (ΔNO$_{2Amm}$ = 420 − 40 = 380 ppm). Accordingly, the total N$_2$ formed by reactions (2) and (3) should amount to 80 + 190 = 270 ppm, which is close enough to the 280 ppm of nitrogen actually detected at steady state. Furthermore, the observed lack of 320 ppm in the atomic N balance is compatible with the expected formation of approximately 180 ppm of NH$_4$NO$_3$ due to reaction (3), after subtracting 10 ppm of N$_2$O from the NH$_4$NO$_3$ decomposition. Based on these findings, we therefore propose that both reactions (2) and (3) occurred during the first stage of the transient run in Fig. 5, with the formation and deposition of ammonium nitrate on Fe-ZSM5. Again, the same behavior had been reported previously under similar conditions over V$_2$O$_5$–WO$_3$/TiO$_2$ and zeolite catalysts [4,6,7,10,21,26].

We now examine the second stage of the TRM run in Fig. 5. When NO$_2$ was removed from the feed stream at $t \approx 13,000$ s, a discontinuity in the outlet concentration traces of all species but NO became apparent. In fact, the ammonia concentration rose to about 960 ppm, the NO$_2$ trace dropped rapidly to zero, the N$_2$ concentration decreased to about 60 ppm (mirroring the NH$_3$ evolution), and the NO outlet concentration remained unaltered at 460 ppm. For pseudo steady-state conditions, such data imply similar consumption of NO and NH$_3$ (about 40 ppm) and a simultaneous formation of 60 ppm of N$_2$, demonstrating a stoichiometry similar to that reported earlier for the reaction between NO and NH$_4$NO$_3$ [reaction (6)]. In other words, during this second stage of the experiment, NO was reacting with the ammonium nitrate deposited onto the catalyst for the duration of the first stage. The resulting transient lasted about 6000 s and in fact ended after depletion of all of the previously accumulated ammonium nitrate.

We now analyze in more detail the chemistry before and after NO$_2$ was removed from the feed. We have shown that the conversion of NO was due to the fast SCR reaction (2) when NH$_3$, NO, and
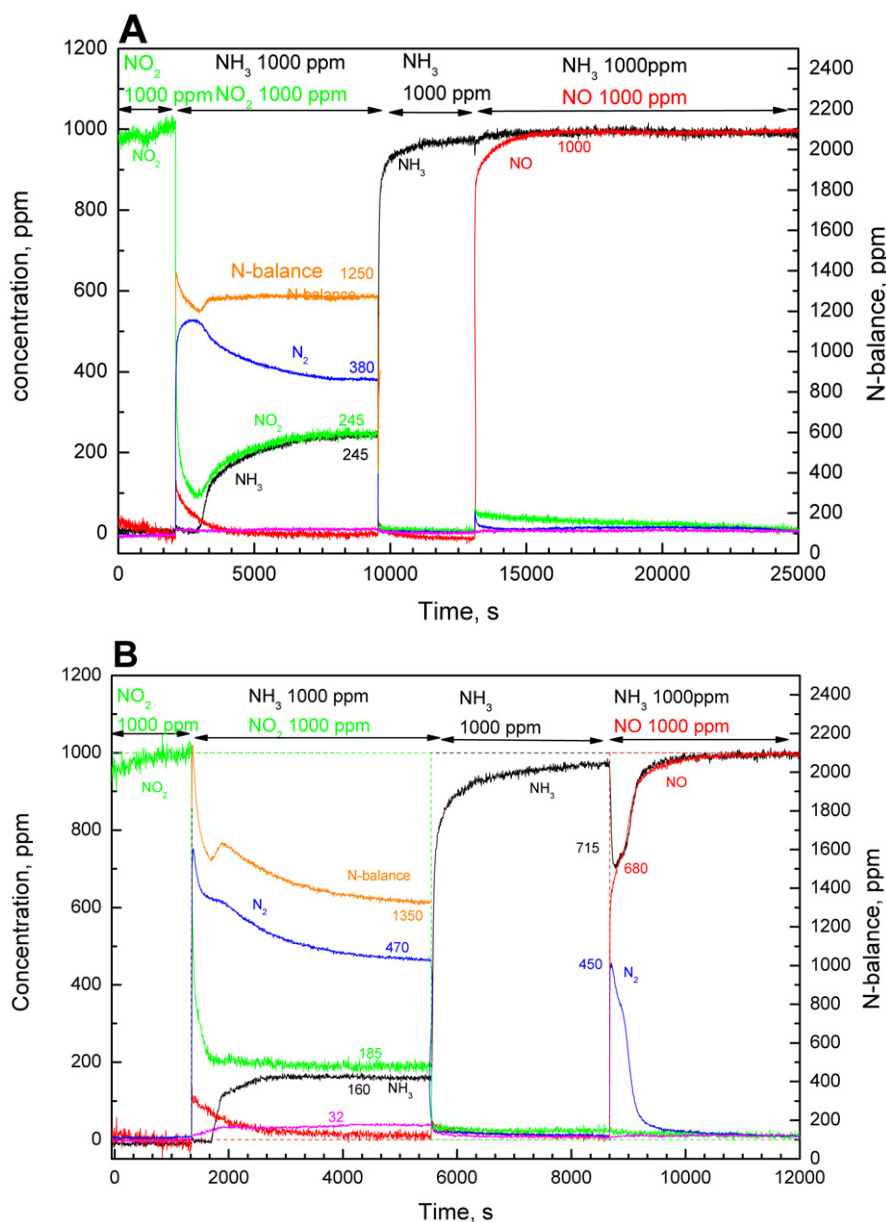
Fig. 4. Effect of temperature on the buildup of ammonium nitrate and its reactivity with NO over Fe-ZSM5. $W_{cat} = 0.080$ g, flow rate $= 72$ cm^3/min (STP). Feed $= 1\%$ H$_2$O, 0% O$_2$, NH$_3 = 0$–1000 ppm, NO $= 0$–1000 ppm, NO$_2 = 0$–1000 ppm + He. $T = 150\,°$C (A), $190\,°$C (B).

NO$_2$ were co-fed to the Fe-ZSM5 catalyst. In contrast, in the subsequent stage, in the absence of NO$_2$, NO consumption was due to reaction (6) between NO and ammonium nitrate. But despite the occurrence of two formally different reactions, the experimental concentration trace of NO shown in Fig. 5 demonstrates no discontinuity between the two stages on the stepwise removal of NO$_2$ from the feed stream. However, recalling that in the presence of NH$_3$, NO, and NO$_2$ (first stage in Fig. 5), the formation of ammonium nitrate [reaction (3)] was already active along with the fast SCR reaction (2), this apparent contradiction can be explained by considering that during the first stage of the run, NO consumption occurred not directly at the expense of gaseous NO$_2$ [i.e., according to reaction (2)], but rather via reaction of NO with NH$_4$NO$_3$ [i.e., according to reaction (6)], with ammonium nitrate in turn formed from NO$_2$ and NH$_3$ according to reaction (3). This obviously explains the absence of any discontinuity of the NO trace between the two parts of the experiment shown in Fig. 5 and points to a sequential scheme for the fast SCR chemistry in which ammonium

nitrate (or a related surface species) plays the role of the key intermediate and reaction (6) between NO and ammonium nitrate is the rate-determining step at these low temperatures. In particular, we emphasize that the data shown in Fig. 5 demonstrate the occurrence of the fast SCR in the absence of gaseous NO$_2$ and rule out significant contributions to deNO$_x$ activity from a direct gas-phase reaction between NO and NO$_2$ [16]. These conclusions regarding the fast SCR chemistry over Fe-ZSM5 are in close agreement with our previous findings for a V$_2$O$_5$–WO$_3$/TiO$_2$ catalyst [6,7].

We further investigated the role of reaction (6) between NH$_4$NO$_3$ and NO in the fast SCR chemistry over the Fe-zeolite at other temperatures, 150 and 190 °C; the results are shown in Fig. 6. At the end of the first stage of the TRM run at 150 °C (Fig. 6A), we observed no conversion of NO and equimolar conversions of NH$_3$ and NO$_2$ (ΔNH$_3 = 410$ ppm, ΔNO$_2 = 405$ ppm), resulting in the evolution of 200 ppm of N$_2$ and a lack of 400 ppm in the N balance. These data indicate the occurrence of reaction (3) (formation of ammonium nitrate) only, whereas the absence of NO conver-
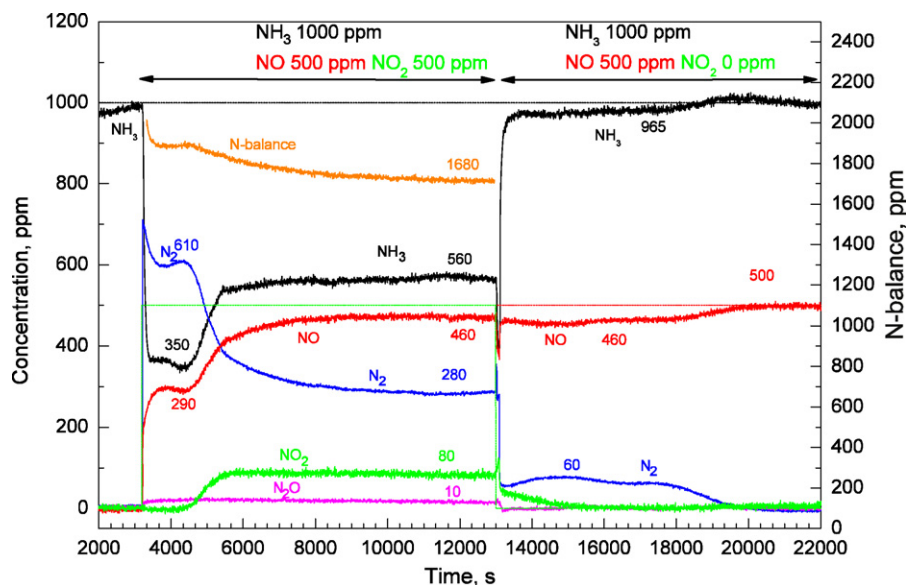
Fig. 5. Comparison between activity of fast SCR and activity of NO + NH$_4$NO$_3$ over Fe-ZSM5. W_{cat} = 0.080 g, flow rate = 72 cm^3/min (STP). Feed = 1% H$_2$O, 0% O$_2$, NH$_3$ = 0–1000 ppm, NO = 0–500 ppm, NO$_2$ = 0–500 ppm + He. T = 170 °C.

sion is explained by the adverse effect of low temperature on the reactivity between NO and NH$_4$NO$_3$, as discussed previously (see Fig. 4A). In fact, no reactivity of NO was detected during the subsequent transient phase after NO$_2$ was removed from the feed.

In contrast, the first stage of the TRM run at 190 °C (Fig. 6B) resulted in high equimolar conversions of NH$_3$ and NO$_x$ (about 95%) associated with higher consumption of NO$_2$ compared with NO ($\triangle$NO$_2$ = 500 ppm, $\triangle$NO = 445 ppm), formation of 915 ppm of N$_2$, and a lack of about 40 ppm in the atomic N balance. Within the limits of experimental error, such data are again consistent with the simultaneous occurrence of ammonium nitrate formation (3) and the fast SCR reaction (2), although with a much greater contribution of the latter than occurred at 170 °C. This finding is explained by the strong promoting effect of temperature on the key reaction (6) between NO and NH$_4$NO$_3$ documented in Figs. 3 and 4.

The subsequent TRM stage, run at 190 °C after NO$_2$ removal, demonstrated significant conversion of NO and NH$_3$, but only during an initial short transient phase. This finding is linked to the high fast SCR activity and the low NH$_4$NO$_3$ production observed during the preceding stage in the presence of NH$_3$, NO, and NO$_2$. Accordingly, at 190 °C, the system was unable to build up a substantial amount of ammonium nitrate on the catalyst for its subsequent reaction with NO in the absence of NO$_2$, thus confirming the importance of NH$_4$NO$_3$ in the NO–NO$_2$/NH$_3$ chemistry at low temperatures.

3.4. NH$_3$ inhibition of NO reactivity with nitrates

Additional interesting information can be extracted from the final part of the TRM run at 150 °C. As shown in Fig. 6A, immediately after the NH$_3$ feed was shut off (t > 24,000 s), a peak of deNO$_x$ activity involving conversion of NO, formation of N$_2$, and evolution of NO$_2$ appeared. The transient exhibited two distinct phases. In the first phase, NO conversion was associated with equimolar formation of N$_2$ and NO$_2$, consistent with reaction (6) between NO and the residual ammonium nitrate on the catalyst surface,

$$NH_4NO_3 + NO \rightarrow N_2 + NO_2 + 2H_2O. \tag{6}$$
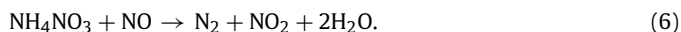
In the second phase, however, the outlet concentration of N$_2$ was greater than that of NO$_2$. This can be explained by a further reaction of NO$_2$ from reaction (6) with NH$_3$ still adsorbed onto the

catalyst according to reaction (3). Thus, the behavior observed at the time of ammonia shutoff is consistent with the overall fast SCR chemistry proposed over Fe-ZSM5, but apparently contradicts the temperature threshold of 150 °C observed for the onset of reaction (6) between NH$_4$NO$_3$ and NO. A possible reason for this finding is that reaction (6) actually may occur between NO and nitric acid (or surface nitrates) [see reaction (11)] formed by NH$_4$NO$_3$ decomposition according to reaction (10 reverse), and then would be inhibited by NH$_3$. Reducing the gaseous ammonia concentration would shift the equilibrium of NH$_4$NO$_3$ decomposition toward higher HNO$_3$ concentrations, thereby promoting the reactivity with NO. A similar effect was observed at different temperatures as well. The formation of surface nitrates and their role in the formation of ammonium nitrate were already demonstrated in this work by the NO$_2$ adsorption experiments (see Fig. 2). Ammonia inhibition of reaction (6) over V$_2$O$_5$–WO$_3$/TiO$_2$ also has been proposed [6,7].

3.5. TPR experiments

More information confirming the central role of nitrates in the fast SCR reactivity is provided in Fig. 7, which compares the temperature dependence of NO conversion measured during four different NO + NH$_3$ TPR experiments with equal space velocities and heating rates (20 K/min). In the experiment reflected in curve A, the feed included NO + NH$_3$ (1000 ppm each) + H$_2$O (1% v/v), but no oxygen. As expected, the observed temporal evolution of the outlet concentrations, indicating the onset of deNO$_x$ activity only above 300 °C, is in agreement with the so-called "slow" SCR reaction [4], that is, the poorly active deNO$_x$ reaction between NO and NH$_3$ in the absence of oxygen,

$$3NO + 2NH_3 \rightarrow \frac{5}{2}N_2 + 3H_2O. \tag{14}$$
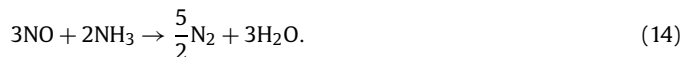
Repeating the same temperature ramp experiment but with 2% O$_2$ v/v in the feed (curve B) revealed greater deNO$_x$ activity, due to the standard SCR reaction (1) instead of reaction (14). Curve C shows the even much higher deNO$_x$ activity resulting from running the same temperature ramp with a feed containing 1000 ppm of NH$_3$ and 500 ppm each of NO and NO$_2$. Of course, curve C is representative of the NO conversion in the fast SCR reaction (2). During the fourth and final TPR experiment, associated with curve D, a feed containing NO + NH$_3$ (1000 ppm each) + H$_2$O (1% v/v), but no
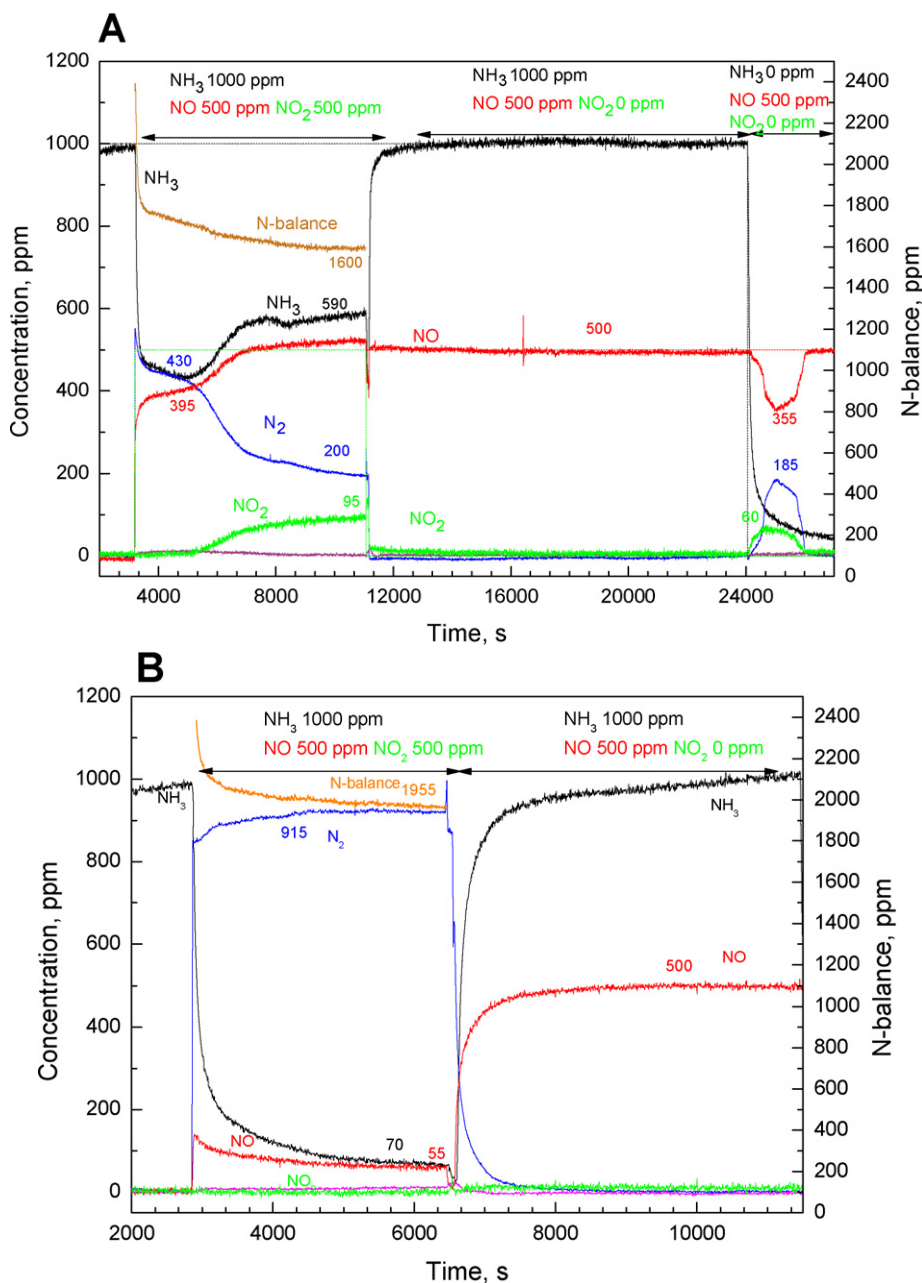
Fig. 6. Comparison between activity of fast SCR and activity of NO + NH$_4$NO$_3$ over Fe-ZSM5: effect of temperature. W_{cat} = 0.080 g, flow rate = 72 cm^3/min (STP). Feed = 1% H$_2$O, 0% O$_2$, NH$_3$ = 0–1000 ppm, NO = 0–500 ppm, NO$_2$ = 0–500 ppm + He. T = 150 °C (A), 190 °C (B).

oxygen or NO$_2$, was passed over a catalyst sample preexposed to 1000 ppm of NO$_2$ + 1% H$_2$O at 60 °C. Fig. 7 shows that during the initial part of this temperature ramp, up to about 200 °C, the evolution of the NO conversion matched that seen for the fast SCR TPR run. As the experiment proceeded, NO conversion dropped sharply, reaching close to zero, before eventually approaching the behavior observed for the slow SCR reaction (curve A).

Recalling the data on the buildup of nitrates on the Fe-ZSM5 catalyst on NO$_2$ adsorption (see Fig. 2), a likely explanation of the similarity between the initial parts of curves C (fast SCR) and D (NO + NH$_3$ over catalyst pretreated with NO$_2$) in Fig. 7 is that in both cases, NO and ammonia in the feed were reacting with surface nitrates, either formed directly via NO$_2$ disproportion (curve C) or formed previously and stored on the catalyst during its pretreatment with NO$_2$ (curve D). Notably, once again in this experiment, the deNO$_x$ activity in the absence of gaseous NO$_2$ but

the presence of surface nitrates was virtually identical to that associated with the fast SCR reaction up to about 200 °C. The drop in NO conversion shown by curve D at temperatures above 200 °C can be attributed to the depletion of surface nitrates. In fact, in another similar experiment (not reported), in which the catalyst was pretreated with NO$_2$ at 150 °C rather than at 60 °C, an earlier drop of the NO conversion occurred, due to the reduced amount of nitrates stored at the higher temperature. Eventually, the match between curves D and A at temperatures above 300 °C confirms the absence of any residual oxidizing agents in the final part of the temperature ramp experiment over the NO$_2$-pretreated sample.

Based on the data presented and discussed so far, the reactivity of NO/NO$_2$–NH$_3$ over Fe-ZSM5 at low temperatures appears to be totally consistent with earlier findings over vanadium-based catalysts [6,7,23] as well as with the mechanistic proposals for
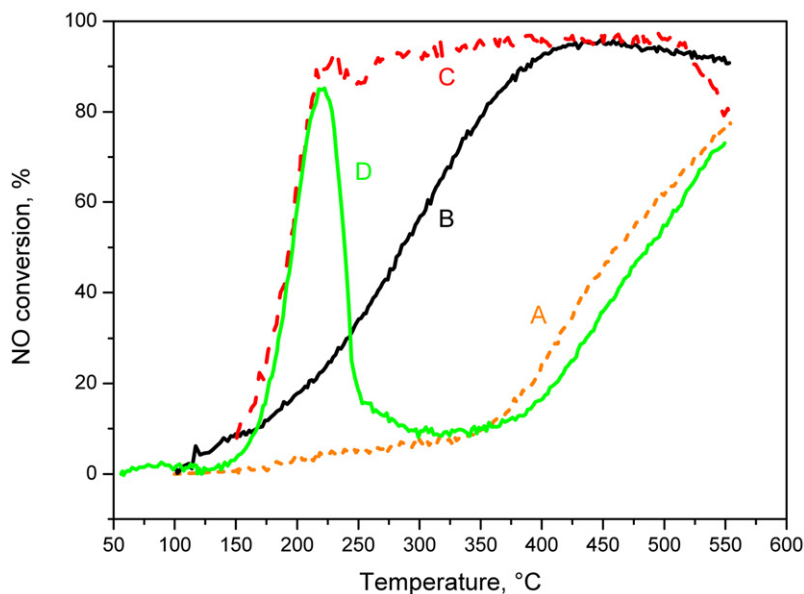
Fig. 7. Temperature-programmed reaction experiments over Fe-ZSM5. $W_{cat} = 0.080$ g, flow rate = 72 cm^3/min (STP). Curve A (slow SCR): Feed = 1% H$_2$O, 0% O$_2$, NH$_3$ = 1000 ppm, NO = 1000 ppm + He. Curve B (standard SCR): Feed = 1% H$_2$O, 2% O$_2$, NH$_3$ = 1000 ppm, NO = 1000 ppm + He. Curve C (fast SCR): Feed = 1% H$_2$O, 0% O$_2$, NH$_3$ = 1000 ppm, NO = 500 ppm, NO$_2$ = 500 ppm + He. Curve D: Feed = 1% H$_2$O, 0% O$_2$, NH$_3$ = 1000 ppm, NO = 1000 ppm + He over catalyst pretreated with NO$_2$ (1000 ppm) + H$_2$O (1%) at 60 °C.
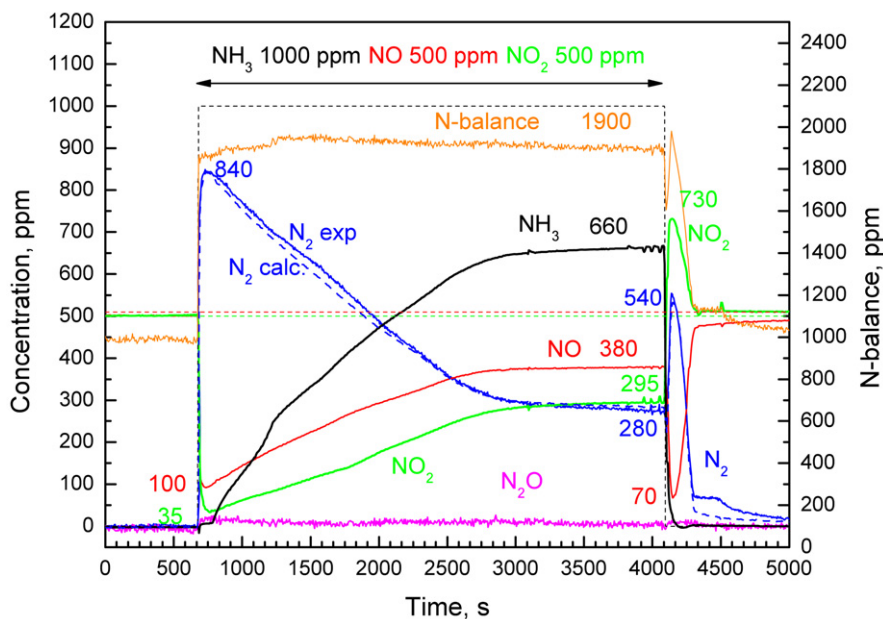
Fig. 8. Fast SCR: TRM run over Fe-ZSM5. $W_{cat} = 0.100$ g, flow rate = 240 cm^3/min (STP). Feed = 1% H$_2$O, 2% O$_2$, NH$_3$ = 0–1000 ppm, NO = 0–500 ppm, NO$_2$ = 0–500 ppm + He. $T = 200$ °C.

BaNa–Y [18], all of which depend on the reactivity between NO and ammonium nitrate or surface nitrates in the fast SCR chemistry. Our findings further demonstrate the similarity of the rate of the fast SCR reaction and the rate of nitrate reduction by NO, which had not been reported previously on zeolite catalysts.

3.6. Fast SCR dynamics under NH$_3$ pulsed feed

We analyzed the dynamic behavior of the NO/NO$_2$–NH$_3$ reacting system over Fe-ZSM5 under a stepwise feed of ammonia at low temperature at conditions closer to those prevailing in real automotive SCR converters—namely in the presence of oxygen and at higher space velocities. Fig. 8 shows the temporal evolution of the outlet species concentrations during a TRM run at

200 °C with 1000 ppm of NH$_3$ added to a feed stream containing 500 ppm of NO and 500 ppm of NO$_2$ with O$_2$ (2%) and H$_2$O (1%). The data identify a first transient phase with high deNO$_x$ activity that was, however, progressively reduced until steady state was reached, along with a final phase after NH$_3$ shutoff, again associated with high deNO$_x$ activity, which was rapidly exhausted. Fig. 8 shows a simultaneous conversion of both NO and NO$_2$ at steady state at the end of the first phase, with NO$_2$ consumption higher by about 100 ppm, formation of N$_2$ in amounts equal to 3/2 of the NO consumption added to half of the NO$_2$ consumption, and a lack of 100 ppm in the N balance. Such behavior can be well explained by the chemistry discussed in the previous sections, invoking ammonium nitrate formation [reaction (3)] and the consecutive reaction (6) between NO and NH$_4$NO$_3$.

Somewhat different behavior can be observed in the second phase of the run shown in Fig. 8. After stepwise removal of NH$_3$ from the feed, a peak in NO conversion appeared, accompanied by evolution of N$_2$ and of NO$_2$, which temporarily exceeded their feed concentrations of 500 ppm. In analogy to the discussion of the final stage in Fig. 6A, such dynamics can be attributed to the reaction of NO with ammonium nitrate and to the inhibiting effect of ammonia. In fact, removing NH$_3$ from the gas phase promoted reaction (6) between NO and NH$_4$NO$_3$ still present on the catalyst, thereby releasing NO$_2$ and N$_2$ until the surface species was depleted.

More TRM runs at higher temperatures (225–300 °C) (not reported) demonstrated higher activity, approaching total conversion of NO$_x$. The reaction dynamics observed during the first stage of the TRM runs, after the addition of NH$_3$ to the feed stream, were qualitatively similar to the run shown in Fig. 8, but transients were faster due to the higher deNO$_x$ activity. In contrast, the final transient phase after the removal of NH$_3$ from the feed became shorter with increasing temperature, and eventually disappeared. This is consistent with the reduced storage of surface species (adsorbed NH$_3$ and nitrates) at higher temperatures.

3.7. Rephrasing the reactions in terms of surface species

Throughout this paper, all of the reactions involved in the NO–NO$_2$/NH$_3$ chemistry have been expressed conventionally in terms of molecular species. But, as is apparent from the data presented so far, the actual catalytic mechanism likely involves related surface adspecies, as discussed, for example, in the analysis of the data given in Figs. 6 and 7. Accordingly, HONO and HNO$_3$ in the reaction steps should be replaced with nitrite and nitrate species, respectively.

Fig. 9 shows a schematic summary of the fast SCR chemistry in terms of surface species. The related basic reaction steps are given in Table 1, along with data on the decomposition of the overall reactions observed in this work. Thus, for example, the reaction sequence yielding the fast SCR reaction (2) can be rephrased in terms of the elementary steps in Table 1 as
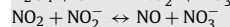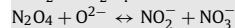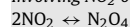
$$2NH_3 + H_2O \leftrightarrow 2NH_4^+ + O^{2-}, \qquad \text{R4}$$

$$2NO_2 + O^{2-} \leftrightarrow NO_2^- + NO_3^-, \qquad \text{R1 + R2}$$

$$NO_3^- + NO \leftrightarrow NO_2 + NO_2^-, \qquad \text{R7}$$
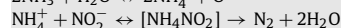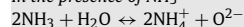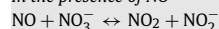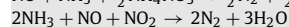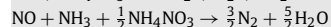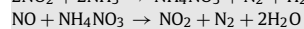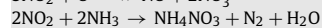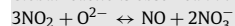
$$2NH_4^+ + 2NO_2^- \rightarrow 2N_2 + 4H_2O. \qquad 2\text{*R5}$$

4. Conclusion

Our findings demonstrate conclusively that the chemistry proposed for the fast SCR reaction at low temperatures over V$_2$O$_5$–WO$_3$/TiO$_2$ [6,7,10,23] and over zeolite systems [13,18,22] is able to interpret the steady-state and dynamic features of the NO/NO$_2$–NH$_3$ system over commercial Fe-ZSM5 catalysts, as well under conditions representative of diesel exhaust after treatment, as proposed previously [23]. Accordingly, the role of NO$_2$ in the fast SCR reactivity is to form surface nitrites and nitrates via dimerization and disproportionation/heterolytic chemisorption, the role of NO is to reduce nitrates to nitrites, and the role of NH$_3$ is to enable rapid and selective decomposition of nitrites to nitrogen via formation of unstable ammonium nitrite. It was pointed out previously that this chemistry can explain the optimal 1:1 molar ratio of NO and NO$_2$ in the fast SCR reaction [6,13,15]. It also can explain the full range of selectivity resulting from varying the NO$_2$/NO$_x$ feed ratio [13,24,26]; incomplete reduction of nitrates by NO (the critical step R7 in Table 1) is responsible for the undesired formation of NH$_4$NO$_3$ at very low temperatures and of N$_2$O at low to intermediate temperatures.

Although the general SCR chemistry emerging from the present work essentially confirms existing concepts, here for the first time it has been evaluated over zeolite systems on a step-by-step basis by means of transient reaction analysis. Thanks to this powerful technique, additional novel results have been obtained over Fe-ZSM5:

1. The reduction of nitrates by NO (or, conversely, the oxidation of NO by nitrates) is the rate-limiting step in the fast SCR chemistry at low temperature; the reverse reaction (i.e., oxidation of nitrites by NO$_2$) is very fast even at very low temperature.

Fig. 9. Proposed reaction scheme for NO/NO$_2$–NH$_3$ SCR at low temperature.
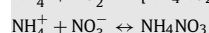
Table 1
The fast SCR chemistry

Basic reaction steps in NO/NO$_2$–NH$_3$ SCR chemistry over V-based and zeolite catalysts	
Involving NO$_2$ only	
$2NO_2 \leftrightarrow N_2O_4$	R1 see (7)
$N_2O_4 + O^{2-} \leftrightarrow NO_2^- + NO_3^-$	R2 see (8)
$NO_2 + NO_2^- \leftrightarrow NO + NO_3^-$	R3 see (11 reverse)
In the presence of NH$_3$	
$2NH_3 + H_2O \leftrightarrow 2NH_4^+ + O^{2-}$	R4 NH$_3$ adsorption
$NH_4^+ + NO_2^- \leftrightarrow [NH_4NO_2] \rightarrow N_2 + 2H_2O$	R5 see (9)
$NH_4^+ + NO_3^- \leftrightarrow NH_4NO_3$	R6 see (10)
In the presence of NO	
$NO + NO_3^- \leftrightarrow NO_2 + NO_2^-$	R7 see (11)
Global reactions observed in this work, and their relationship with the basic reactions above	
$3NO_2 + O^{2-} \leftrightarrow NO + 2NO_3^-$	(12) = R1 + R2 + R3
$2NO_2 + 2NH_3 \rightarrow NH_4NO_3 + N_2 + H_2O$	(3) = R1 + R2 + R4 + R5
$NO + NH_4NO_3 \rightarrow NO_2 + N_2 + 2H_2O$	(6) = R6 reverse + R7 + R5
$NO + NH_3 + \frac{1}{2}NH_4NO_3 \rightarrow \frac{3}{2}N_2 + \frac{5}{2}H_2O$	(13) = (6) + $\frac{1}{2}$*(3)
$2NH_3 + NO + NO_2 \rightarrow 2N_2 + 3H_2O$	(2) = R4 + R1 + R2 + R7 + 2*R5

2. Ammonia inhibits such a redox step, likely by blocking the surface nitrates; high NH_3 concentrations have a detrimental effect on fast SCR kinetics at low temperature [26].
3. The same enhanced fast SCR deNO$_x$ activity also is seen in the absence of gaseous NO_2, provided that the catalyst has been saturated with nitrates. This important result is not obvious from the previous SCR literature.

In summary, our work emphasizes the key role of surface nitrates in the fast SCR chemistry. Their reactivity with NO is critical to explaining the strongly enhanced deNO$_x$ activity and governs the fast SCR kinetics at low temperature, whereas their buildup and depletion controls the SCR dynamics in parallel to ammonia adsorption–desorption. Identifying the elementary steps of fast SCR reactions over the Fe-ZSM5 catalyst is an important step in deriving chemically consistent kinetic schemes, as well as a key stage in the development of new catalytic systems and integrated aftertreatment technologies.

Acknowledgments

References

[1] G. Madia, M. Koebel, M. Elsener, A. Wokaun, Ind. Eng. Chem. Res. 41 (2002) 3512.
[2] M. Koebel, M. Elsener, G. Madia, Ind. Eng. Chem. Res. 40 (2001) 52.
[3] M. Koebel, G. Madia, F. Raimondi, A. Wokaun, J. Catal. 209 (2002) 159.
[4] M. Koebel, G. Madia, M. Elsener, Catal. Today 73 (2002) 239.
[5] C. Ciardelli, I. Nova, E. Tronconi, D. Chatterjee, T. Burkhardt, M. Weibel, Chem. Eng. Sci. 62 (2007) 5001, and references therein.
[6] C. Ciardelli, I. Nova, E. Tronconi, D. Chatterjee, B. Bandl-Konrad, Chem. Commun. (2004) 2718.
[7] I. Nova, C. Ciardelli, E. Tronconi, D. Chatterjee, B. Blandl-Konrad, Catal. Today 114 (2006) 3.
[8] E. Tronconi, I. Nova, C. Ciardelli, D. Chatterjee, M. Weibel, J. Catal. 245 (2007) 1.
[9] I. Nova, C. Ciardelli, E. Tronconi, D. Chatterjee, M. Weibel, Top. Catal. 42–43 (2007) 43.
[10] C. Ciardelli, I. Nova, E. Tronconi, B. Bandl-Konrad, D. Chatterjee, M. Weibel, B. Krutzsch, Appl. Catal. B: Environ. 70 (2007) 80.
[11] K. Rahkamaa-Tolonen, T. Maunula, M. Lomma, M. Huuhtanen, R. Keiski, Catal. Today 100 (2005) 217.
[12] M. Schwidder, M.S. Kumar, K. Klementiev, M.M. Pohl, A. Brückner, W. Grünert, J. Catal. 231 (2005) 314.
[13] O. Kröcher, M. Devadas, M. Elsener, A. Wokaun, N. Söger, M. Pfeifer, Y. Demel, L. Mussmann, App. Catal. B: Environ. 66 (2006) 208.
[14] M. Wallin, C.J. Karlsson, M. Skoglundh, A. Palmqvist, J. Catal. 218 (2003) 354.
[15] M. Li, Y. Yeom, E. Weitz, W.M.H. Sachtler, J. Catal. 235 (2005) 201.
[16] H. Sjövall, L. Olsson, E. Fridell, R.J. Blint, Appl. Catal. B: Environ. 64 (2006) 180.
[17] G. Delahay, D. Valade, A. Guzma-Vargas, B. Coq, Appl. Catal. B: Environ. 55 (2005) 149.
[18] Y.H. Yeom, J. Henao, M.J. Li, W.M.H. Sachtler, E. Weitz, J. Catal. 231 (2005) 181.
[19] G. Li, C.A. Jones, V.H. Grassian, S.C. Larsen, J. Catal. 234 (2004) 401.
[20] M.S. Kumar, M. Schwidder, W. Grünert, U. Bentrup, A. Brückner, J. Catal. 239 (2006) 173.
[21] J. Despres, M. Koebel, O. Kröcher, M. Elsener, A. Wokaun, Microporous Mesoporous Mater. 58 (2003) 175.
[22] M. Devadas, O. Kröcher, M. Elsener, A. Wokaun, N. Söger, M. Pfeifer, Y. Demel, L. Mussmann, Appl. Catal. B: Environ. 67 (2006) 187.
[23] O. Kröcher, in: Proceedings of Congress MinNO$_x$—Minimization of NO$_x$ Emissions through Exhaust Aftertreatment, Berlin, February 1–2, 2007, Paper H030-02-286-7.
[24] M. Devadas, O. Kröcher, M. Elsener, A. Wokaun, G. Mitrikas, N. Söger, M. Pfeifer, Y. Demel, L. Mussmann, Catal. Today 119 (2007) 137.
[25] V. Sanchez-Escribano, T. Montanari, G. Busca, Appl. Catal. B: Environ. 58 (2005) 19.
[26] A. Grossale, I. Nova, E. Tronconi, Catal. Today (2007), doi:10.1016/j.cattod.2007.10.117.